

LQR and PPM Control of Inverted Pendulum

Ahmed Yousif Enad Al Baaj¹, Zoubeir Tourki²

Department of Mechanical Engineering, University of Soussa, Soussa, Tunisia ^{1,2}

Abstract

The inverted pendulum is a classic control problem in which a pendulum is balanced in an upright position by adjusting the position of the cart on which it is attached. This system is inherently unstable, requiring precise control to keep the pendulum in equilibrium. This thesis investigates the control of an inverted pendulum system using two different methods theoretically (pole placement and linear quadratic control) and experimentally. The major goal is to evaluate the impact of various parameters, such as cart mass, pendulum mass, and damping coefficient, on system behavior and control performance. The study looks at how changing the mass of the cart, the mass of the pendulum, and the damping coefficient affects the system stability, response time, and control effort. The findings provide useful information about the trade-offs between these factors and the performance of the two control approaches.

Keywords: position of cart, pendulum angle, LQR control, PPM control and Inverted pendulum.

1. Introduction

In 1990, the Theory Committee of the International Federation of Automatic Control (IFAC) identified a collection of practical design challenges that may be used to compare new and current control techniques and tools and generate a valid comparison. The committee came up with a list of recommendations. Control issues from the actual world that were used as "benchmark control problems." Then there's the cascade. The inverted pendulum control issue is described as very unstable, and the difficulty grows as the number of variables rises. In terms of the number of linkages Anderson and Pandy (2003) discussed the mechanics of the inverted pendulum briefly. More on the pendulum as a model of stance phase, as well as Buckzek and his crew (2006) [1,2]. The Inverted Pendulum is a well-known control issue in dynamics and control theory, and it's frequently used as a benchmark for evaluating control algorithms (PID controllers, neural networks, fuzzy control, evolutionary algorithms, and so on). The cart-single inverted pendulum system is the most basic example of this system. It also offers a lot of nice features [3]. From missile launchers to Segway's, human walking, and luggage-carrying pendulous, practical uses abound. Buildings that are earthquake-resistant, for example. The mechanics of the Inverted Pendulum are similar to those of a missile or rocket. Because the launcher's centre of gravity is behind the drag centre, it causes aerodynamic drag instability [4].

There are several modern control systems available today that may be utilized in a variety of situations. Non-linear control, optimum control, and adaptive control are examples of control systems. All of these controls, however, are difficult to implement due to the large number of sequences that must be employed in the controller architecture. An inverted pendulum system is one of the simplest control systems, but it is difficult to balance it in an upright vertical position since the pendulum would naturally go down from that posture. In the control field, an inverted pendulum is one of the most researched systems [1,2]. The inverted pendulum's control goal is to have a linear motor swing up the pendulum hinged on the moving cart from a stable position "vertically downstate" to the zero states "vertically upward state" and hold the pendulum there despite an interruption. In control field theory, a pendulum may be characterized as a system [5-7].

A vertical pendulum rod, a horizontal pendulum arm, a motor, and an encoder make up an inverted pendulum. Stephenson created this method over 100 years ago, and the controller is required to accomplish stability for the

inverted pendulum to stay standing [8]. Chao investigated the elasticity of the inverted pendulum in the presence of a beam. This method is extensively used in control engineering and has been implemented in a variety of sectors, including balancing a broom with only one hand, launching a rocket from the ground, and stabilizing a robot arm. As a result, there have been numerous studies on the inverted pendulum system that are still being carried out everywhere [9]. In the control field, the layout of the inverted pendulum comprises several forms of designation. The most common application is on massive lifting cranes in shipyards. The cranes move the shipping containers back and forth in such a way that the box never swings or sways. Even when moving or stopping fast, it always stays properly positioned beneath the operator [10,11]. Without any feedback or control system, another approach to maintain an inverted pendulum is to oscillate the support rapidly up and down. The inverted pendulum may recover from disturbances in a stunningly counterintuitive manner if the oscillation is sufficiently in terms of amplitude and acceleration [12].

The mode of actuation and the number of degrees of freedom were two features of this inverted pendulum configuration. For the technique of actuation, there are two elements to consider linear and rotary inverted pendulum systems. Force, F , is the input for a linear inverted pendulum system, whereas torque, T , is the input for a rotary inverted pendulum system [5,13]. The movement of the cart in the linear configuration of an inverted pendulum is horizontal, which may be controlled by a motor when the pendulum is connected to the cart. The horizontal arm of the rotating inverted pendulum is coupled to the upper surface of the motor as well as the encoder's end. The servo motor drives are connected to the rotating inverted pendulum system, and the position of the angle may be measured using an encoder that acts as a sensor [14]. There are two types of encoders that are used with a pendulum connected to measure the angle of the pendulum. The simulation will subsequently be carried out using real-time software based on Mat lab/Simulink. There were two sorts of pendulum positions: stable and unstable. The position of the pendulum in a vertical upright position indicates that it is in an unstable state, but when it is vertically down, it is in a stable state [15].

2. System Description

2.1 Dynamics of the system

This section applies Newton's law of motion to describe the system dynamics of the inverted pendulum. The dynamics indicate that the system has two degrees of freedom: one governing the linear movement of the cart and the other governing the rotational motion of the pendulum [14].

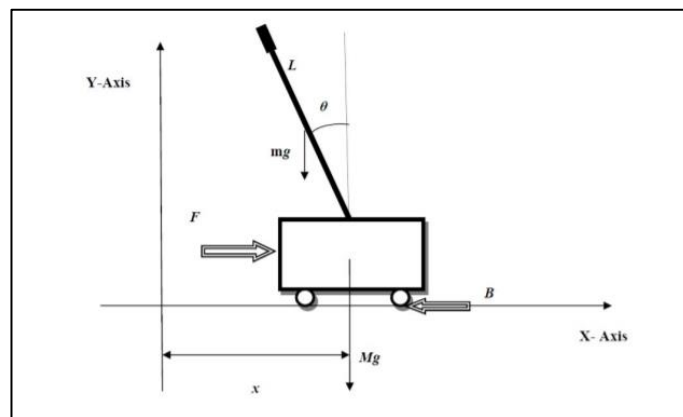


Figure 1. Parametric depiction of Inverted Pendulums [3]

- M refers to Cart mass
- m refers to Pendulum mass
- J refers to Moment of inertia pendulum
- L refers to Pendulum length
- b refers to Cart friction co-efficient

- g refers to Gravitational acceleration

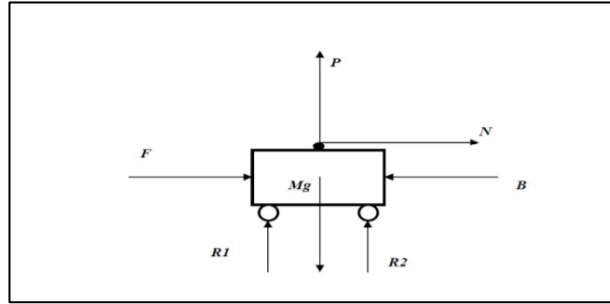


Figure 2. Diagram of an Inverted Pendulum with a Free Body [3]

The analysis focuses solely on horizontal forces because they are the only ones that provide information about the dynamics of the cart, which moves exclusively in a linear path.

$$Ma_x = F + N - B \quad (1)$$

The letter N , the horizontal force exerted by the pendulum on the cart determines the horizontal reaction .

$$N = m \frac{d^2}{dt^2} (x + l \sin \theta) = m\ddot{x} + m\ddot{\theta} l \cos \theta - m(\dot{\theta})^2 l \sin \theta \quad (2)$$

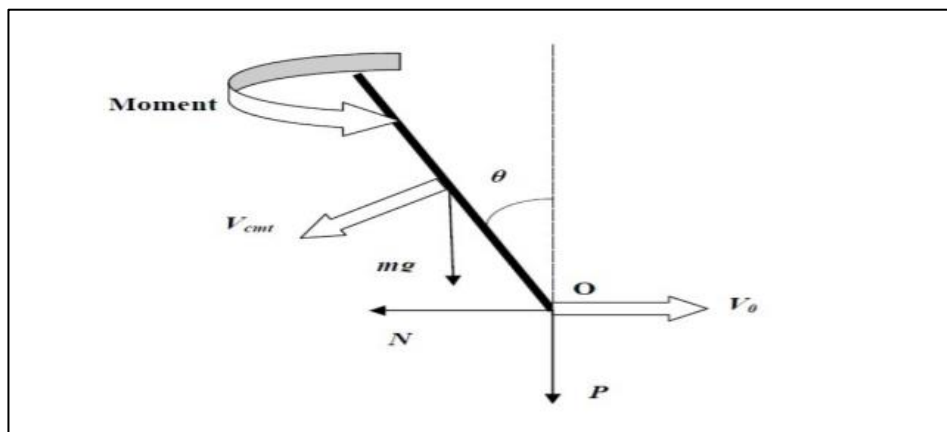


Figure 3. Pendulums free body diagram [4]

P is the vertical force exerted by the pendulum in y direction on the cart . The displacement of the Pendulum from the pivot determines $L \cos \theta$. So

$$P + mg = m \frac{d^2}{dt^2} (l \cos \theta) = m l \ddot{\theta} \sin \theta + m(\dot{\theta})^2 l \cos \theta \quad (3)$$

The velocity of the center of mass is represented by V_{cmt} , V_o denotes the velocity at point o in the direction X , and the sum of moment is :

$$-Nl \cos \theta - Pl \sin \theta = J \ddot{\theta} \quad (4)$$

When we plug in the values for (1.2) and (1.3) into equation (1.4), we obtain

$$Ml\ddot{x} \cos \theta - (ml^2 + J)\ddot{\theta} = -mgl \sin \theta \quad (5)$$

Now, if we replace equation (1.2) for equation (1.1), we obtain

$$\ddot{\theta} = \frac{mL}{\sigma} [(F - b\dot{x}) \cos \theta - m(\dot{\theta})^2 l \cos \theta \sin \theta + (m + M)g \sin \theta] \quad (6)$$

By solving and simplifying equations (1.5) and (1.6), we obtain equations (1.7) and (1.8).

$$\ddot{x} = \frac{1}{\sigma} [(J + ml^2)(F - b\dot{x} - ml\dot{\theta}^2 \sin \theta) + ml^2 g \sin \theta \cos \theta] \quad (7)$$

Where σ is given by

$$\sigma = ml^2 (M + m \cos^2 \theta) + J(M + m) \quad (8)$$

The system's dynamics are described by these two equations.

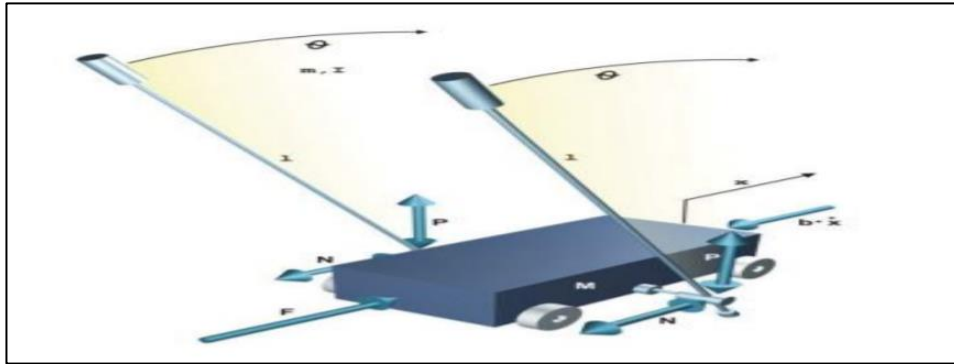


Figure 4. Inverted Pendulum phenomenological model [16]

The phenomenological model (shown in Figure 4) of the pendulum is nonlinear, with one of its states acting as an argument in a nonlinear function [16]. To represent such a model in transfer function form (used in control engineering for linear plant dynamics), it must undergo linearization. The movement of an inverted pendulum is both translational and rotational. Modeling may be done in two ways. The Newtonian approach is the first, while the Lagrangian method is the second. The well-known Newtonian method was applied in this case.

2.2 Linearization

The linearization of non-linear equations is described in this section. Linearize the non-linear equations using tailors series expansion. Assume that we need to stabilize the pendulum angle in the inverted position.

$$\begin{aligned} \theta &\approx 0 \\ \sin \theta &= \theta \\ \cos \theta &= 1 \\ \text{And } \dot{\theta}^2 &= 0 \end{aligned}$$

We get the following after linearizing the equations:

$$\ddot{\theta} = \frac{ml}{\sigma} [(F - b\dot{x}) + (m + M)g\theta] \quad (9)$$

$$\ddot{x} = \frac{1}{\sigma} [(J + ml^2)(F - b\dot{x}) + ml^2 g \theta] \quad (10)$$

$\bar{\sigma}$ denoted by

$$\bar{\sigma} = Mml^2 + J(M + m) \quad (11)$$

In this work, the states that were designed for the advancement of the state model were the pendulum angular velocity ($\dot{\theta}$), cart linear velocity (\dot{x}), cart position (x), and cart position (x). The state space model was used to calculate an inverted pendulum mechanism on a moving car through the equation of motion, which can be written in the form of $\dot{x} = Ax + Bu$ can be represented by:

$$\begin{bmatrix} \dot{x} \\ \ddot{x} \\ \dot{\theta} \\ \ddot{\theta} \end{bmatrix} = \begin{bmatrix} 0 & 1 & 0 & 0 \\ 0 & \frac{(1 + mL^2)b}{\eta} & \frac{(m^2L^2)g}{\eta} & 0 \\ 0 & 0 & 0 & 1 \\ 0 & -\frac{(mLb)}{\eta} & \frac{(M + m)mgL}{\eta} & 0 \end{bmatrix} \begin{bmatrix} x \\ \dot{x} \\ \theta \\ \dot{\theta} \end{bmatrix} + \begin{bmatrix} 0 \\ \frac{(1 + mL^2)}{\eta} \\ 0 \\ \frac{(mL)}{\eta} \end{bmatrix} F \quad (12)$$

$$y = \begin{bmatrix} y_1 \\ y_2 \end{bmatrix} = \begin{bmatrix} 1 & 0 & 0 & 0 \\ 0 & 0 & 1 & 0 \end{bmatrix} \begin{bmatrix} x \\ \dot{x} \\ \theta \\ \dot{\theta} \end{bmatrix} \quad (13)$$

3. Controller Design

One of the most fascinating and fundamental challenges in control engineering is managing an inverted pendulum. This system is designed for students to gain hands-on experience with control theory and practice feedback control in the laboratory. The objective of controlling the inverted pendulum system is to transition the pendulum from its hanging-down state to a stable upright position. Destabilizing controller, stabilizing controller, and mode controller are the three sub-controllers of the controller [17]. The destabilizing controller oscillates the pendulum back and forth until it accumulates enough energy to break the hanging-down stable position and move into the upright unstable position's vicinity. The stabilizing controller then kicks in and keeps the pendulum in the upright unstable position, with the capacity to reject tiny disturbances. When to transition between the destabilizing and stabilizing controllers is determined by, the mode controller Simulation and tests back up the proposed control technique for the inverted pendulum system. According to a qualitative student assessment survey, a modularized control method like this aids students in better understanding control theory [18].

The destabilizing controller, stabilizing controller, and mode controller are the three sub-controllers of the rotary inverted pendulum system's controller. The destabilizing controller oscillates the pendulum back and forth until it accumulates enough energy to break the hanging-down stable position and move into the vicinity of the upright unstable state, as the name suggests [19]. The stabilizing controller is then activated, allowing the pendulum to remain in its upright position. When to transition between the destabilizing and stabilizing controllers is determined by the mode controller [20]. The spinning arm is effectively driven by the destabilizing controller to get the pendulum away from its stable hanging-down position. It's only natural that if the spinning arm is moved back and forth quickly enough, the pendulum would ultimately swing higher. As a result, the initial step is to create a position controller that can swing the rotating arm in order to achieve the destabilizing aim [21].

4. The design of controllers

4.1 Pole Placement Controller

Pole placement is a feedback control system principle that positions the closed-loop poles of a plant at specified locations in the s-plane. This approach is effective because the pole locations directly affect the system's eigenvalues, which in turn dictate its response characteristics. On how to put this approach into action, the system should be regarded controlled. Figure 5. Shows the diagram illustrating the triple inverted pendulum with a pole placement controller [22].

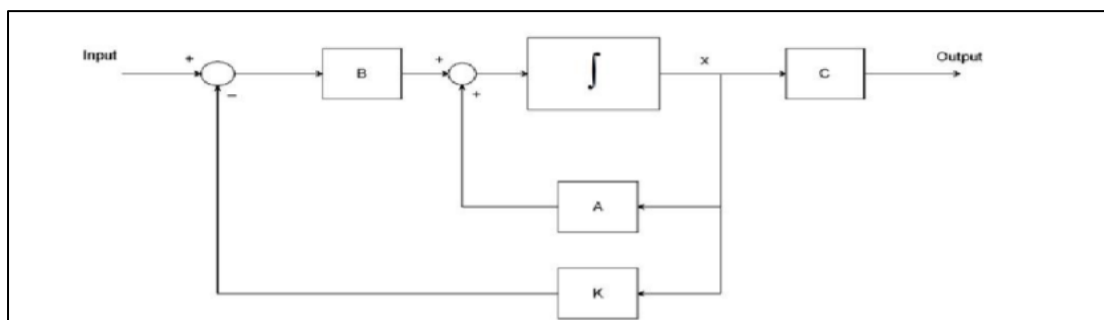


Figure 5. The configuration of the triple inverted pendulum utilizing a pole placement controller [22]

Reviewing the system enables the derivation of state equations for the closed-loop system depicted in Figure 2.3 [22].

$$\dot{x} = Ax + Bu = Ax + B(-K_x) = (A - BK)_x \quad (14)$$

4.2 Linear Quadratic Regulator (LQR):

The Linear Quadratic Regulator (LQR) can only be applied to linear systems represented in state-space form:

$$\dot{x} = Ax + Bu \quad (15)$$

$$y = Cx + Du \quad (16)$$

$$J = 1/2 \int_0^\infty (x^T Qx + u^T Ru) dt \quad (17)$$

Where Q represents the weight matrix for balancing the state variables (also a positive or positive semi-definite matrix) and R denotes the weight matrix for balancing the input variables (also a positive definite matrix). P is the solution to the Riccati equation, obtained through its solution process $PA + A^T P - PBR^{-1}B^T P + Q = 0$, the value of P and the optimum feedback gain matrix $K=R^{-1}B^T P$ may be obtained [23].

4.3 Monte Carlo simulation

Monte Carlo simulation is a computing method that involves repeatedly sampling random variables to evaluate the behavior of a highly nonlinear and complicated system that includes uncertainty. The distribution of data is determined by statistical studies, specifically by calculating the standard deviation (s) and the average value (α) as indicated by:

$$s = \sqrt{\frac{\sum_{i=1}^N (\alpha_i - \bar{\alpha})^2}{N-1}} \quad (18)$$

and,

$$\bar{\alpha} = \frac{1}{N} \sum_{i=1}^N \alpha_i = \frac{\alpha_1 + \alpha_2 + \dots + \alpha_N}{N} \quad (19)$$

The sample item values are represented, with the symbol $\bar{\alpha}$ indicating the mean of these observations. N denotes the total number of observations. The uncertainties in this work pertain to the length of pendulum and its mass, mass of the cart, pendulum, angular location, cart location, and the pendulum angular position.

5. Hardware

For this study, an actual pendulum-cart system was employed. The tools required to regulate motion, exert force, gauge states, and put control schemes into action are included in this system. Figure 6 depicts the system's block diagram, whereas Figure 7 depicts the total system.

A current amplifier, a DC motor with gearing, a cart with a pendulum, a variety of feedback devices, and a computer running Simulink software for signal processing are the many parts that are involved.

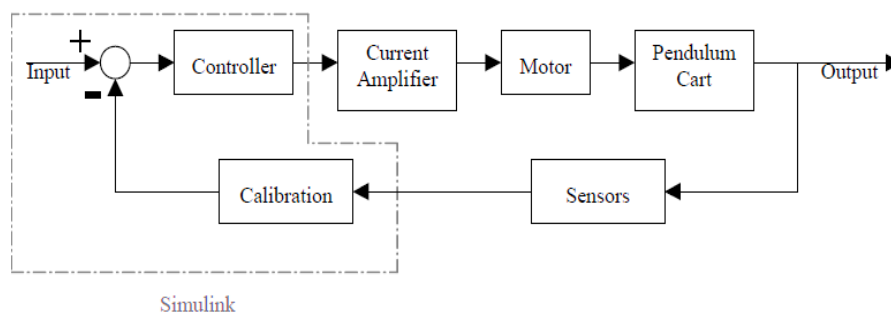


Figure 6. Pendulum Cart System Block Diagram



Figure 7. Photographs of the overall system

6. Time response

Figures (8-13), shows the response. In general, both of the control methods are successfully led the two masses of the system to the desired values in small time duration. However, the system characteristics, such as frequency, over shot, settling time are not similar. For example, LQR method showed smaller overshoot than PPM for the time linear displacement response with smaller steady state time as well. The linear velocity response is also different. PPM showed smaller response for the linear velocities than the corresponding of LQR. This can be attributed to the dramatic change of the linear displacement in LQR response through a smaller duration of time. Still LQR achieve faster response than PPM. This response is noticed for the linear acceleration as well since it depends on the velocity response. However, the situation is the opposite for the angular motion. Less effort is required at PPM to for controlling the angular position of the pendulum, as shown in Figure 11. Although, LQR is faster that PPM to get the steady state response. Smaller overshoot in both angular velocities and angular acceleration of the pendulum are presented by PPM, while both of them lead the pendulum into the desired positions together.

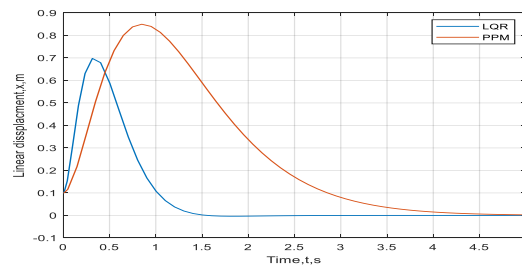


Figure 8. Time response of the linear displacement of the cart for 5 sec

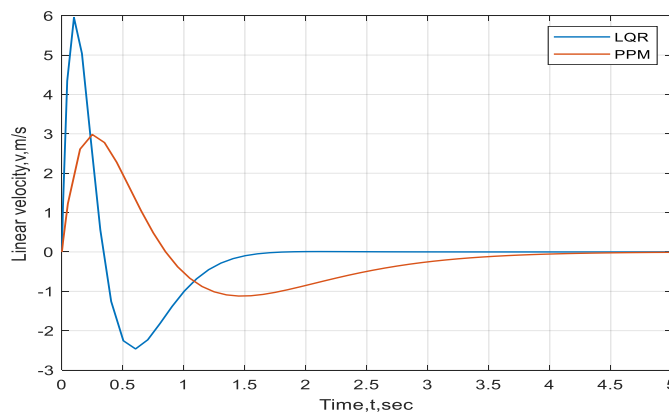


Figure 9. Shows the time response of the linear velocity of the cart over a duration of 5 seconds

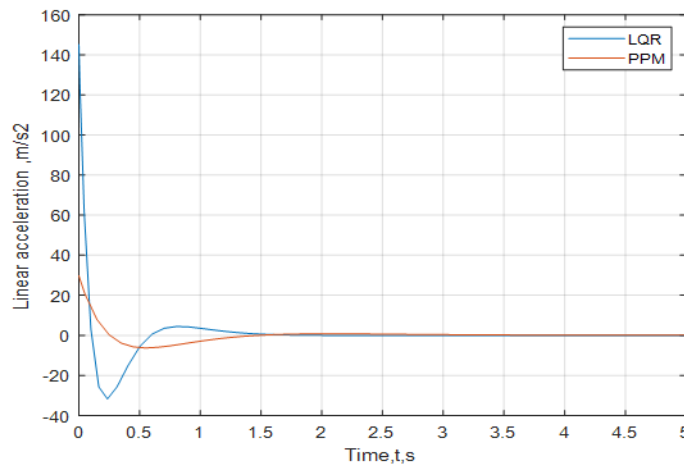


Figure 10. Time response of the linear acceleration of the cart for 5 sec

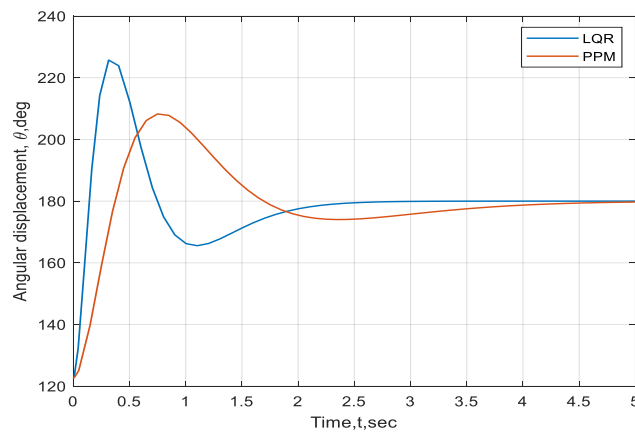


Figure 11. Depicts the time response of the angular displacement of the pendulum over a period of 5 seconds

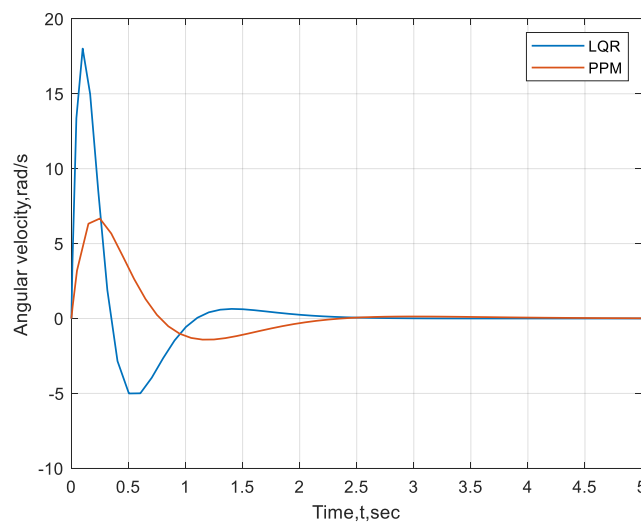


Figure 12. Illustrates the time response of the angular velocity of the pendulum over a duration of 5 seconds

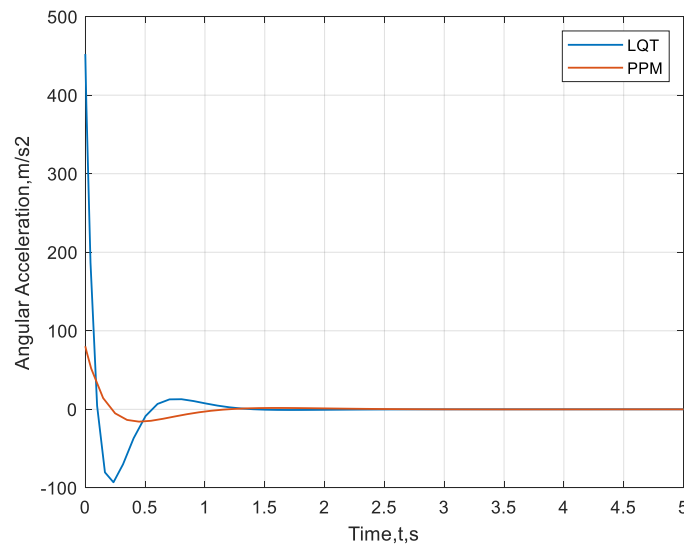


Figure 13. Displays the angular acceleration of the pendulum over a span of 5 sec

7. Parametric Study

7.1 Effect of the Mass of the Cart (M)

The time responses of the system at different mass of the cart are presented in this section, as shown in Figures (14-19). These figures show that variation of the mass of the cart change the overshoot of the time response. However, the steady state time still the same (almost 1.67 sec) the increasing or decreasing is not necessary increase or decrease the time response of the system, due to inertia force of the cart. This situation is completely applicable to the linear and angular displacement, velocity, and acceleration. In addition, the variations in the mass of the cart are not changed the amplitude only, but changed the frequency of the response also. This behavior is attributed to the direct relationship between inertia and system frequency.

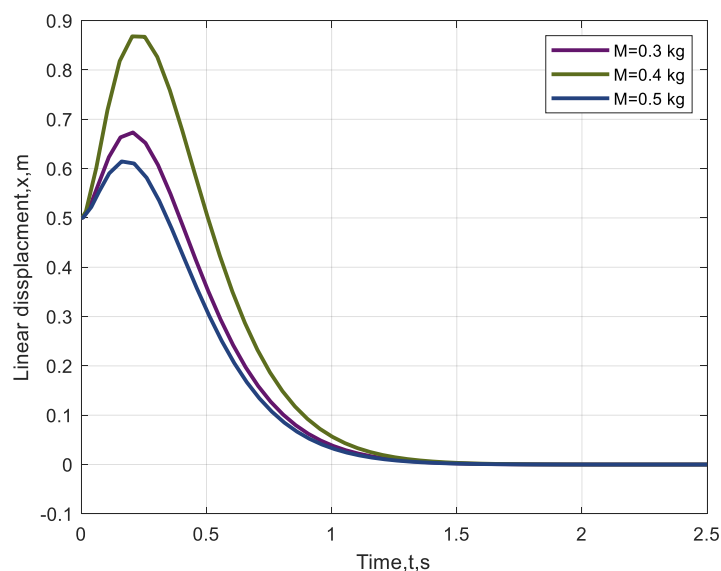


Figure 14. Time response of the linear displacement of the car for different mass of cart

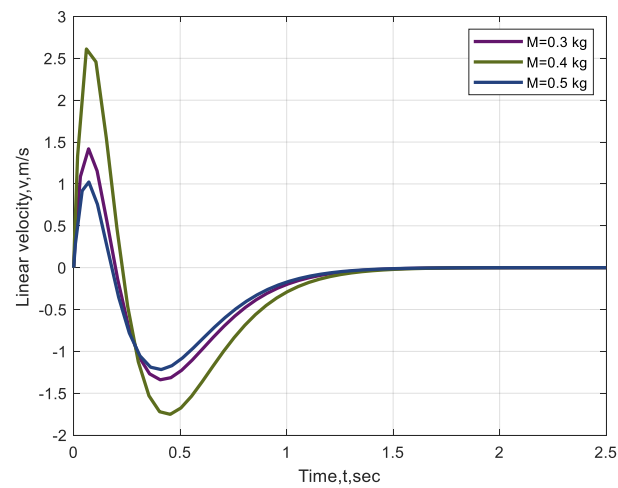


Figure 15. Illustrates the time response of the linear velocity of the car for varying cart

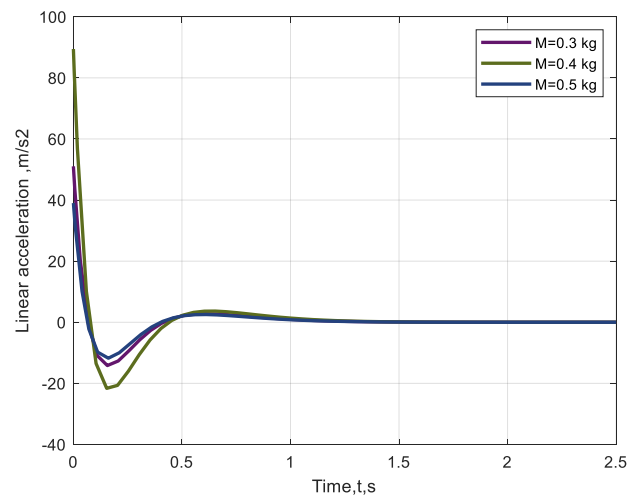
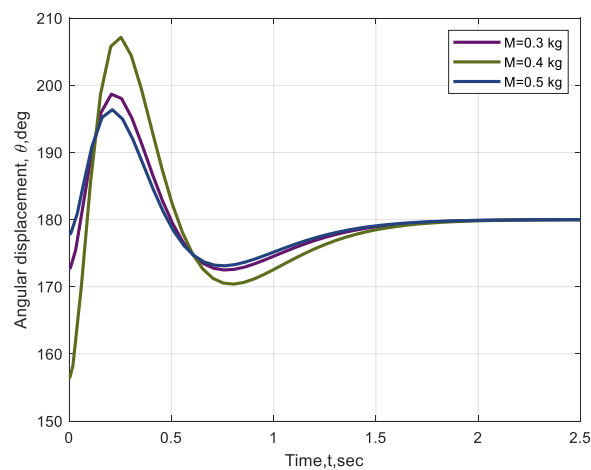


Figure 16. Time response of the linear acceleration of the car for different mass of cart



Figurer 17. Depicts the time response of the angular displacement of the pendulum for different cart masses

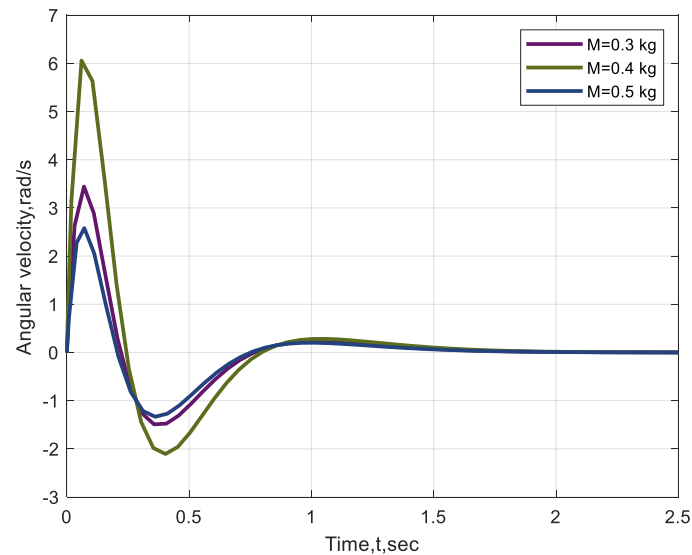


Figure 18. Illustrates the response of the angular velocity of the pendulum for different varying cart masses

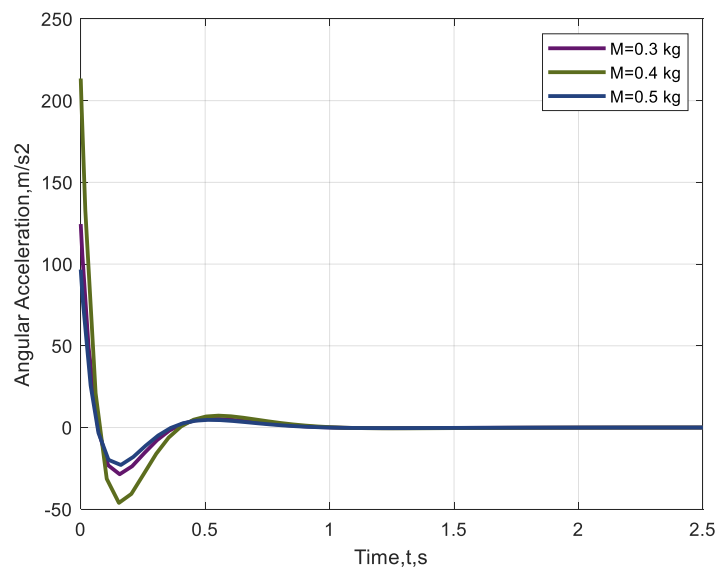


Figure 19. Shows the time response of the angular acceleration of the pendulum for different cart masses.

7.2 Effect of the Mass of the Pendulum (m)

The time responses of the system at different mass of the pendulum are presented in this section, as shown in Figures (20-25). One can notice that the effect of variations in the mass of the pendulum is more prominent on the time response than that corresponding of the variations of the mass of the cart. It is noted that increasing the mass of the pendulum reduces the time response of the cart. This behavior can be attributed to the direct relations between the cart and pendulum in light of action and reaction force. The reaction of the cart for higher pendulum mass is smaller to get to the desired equilibrium or steady state response. Similar analogy is valid for all of the figures mentioned lately.

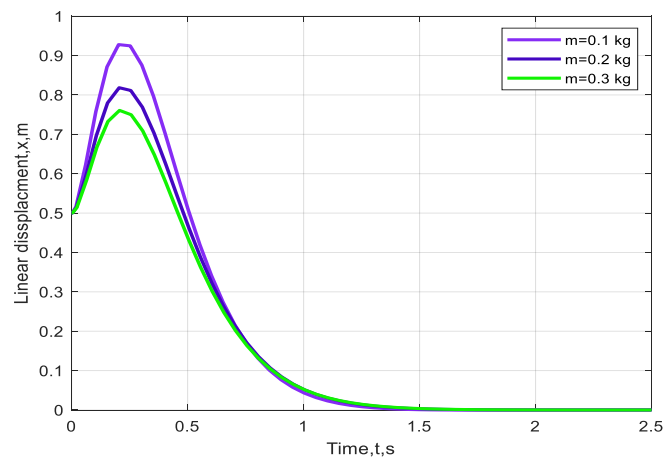


Figure 20. Time response of the linear displacement of the car for different mass of pendulum

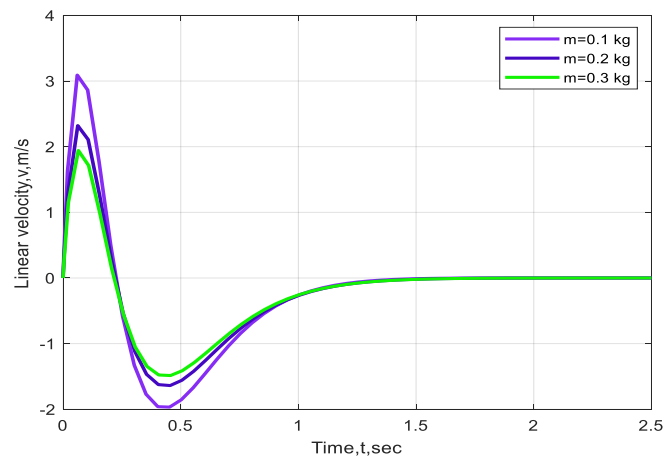


Figure 21. Illustrates the time response of the linear velocity of the cart for varying pendulum masses

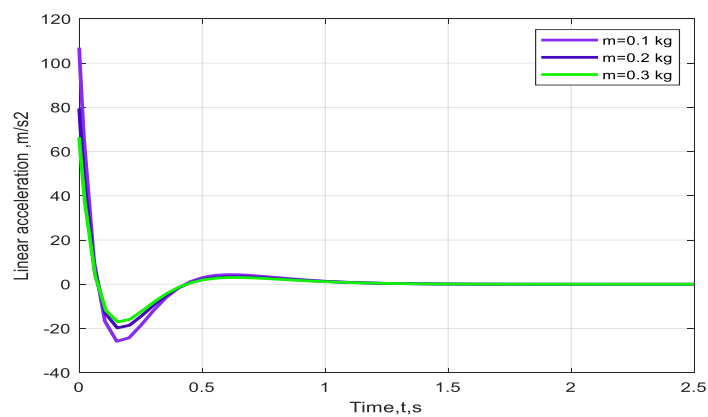


Figure 22. Illustrates the time response of the linear acceleration of the cart for varying pendulum masses

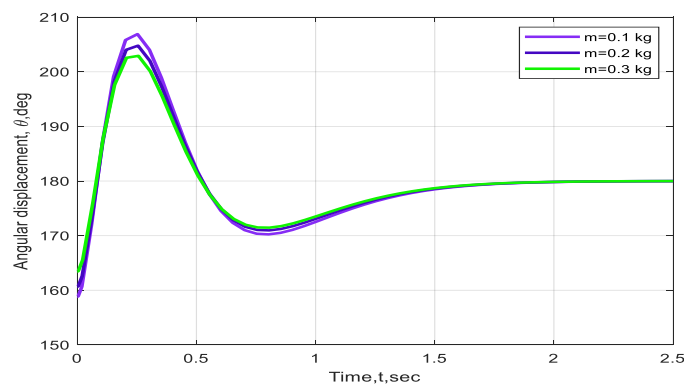


Figure 23. Shows the time response of the rotational displacement of the pendulum for varying pendulum masses

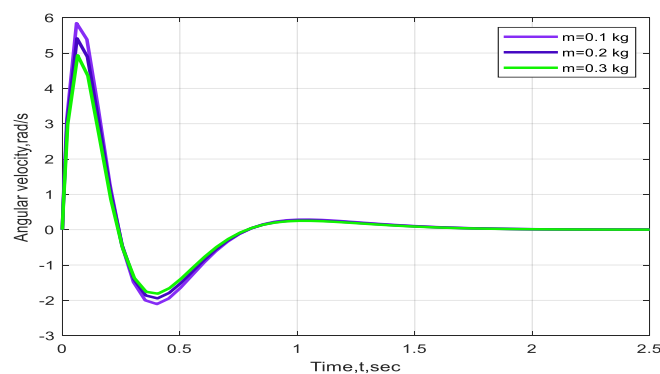


Figure 24. Illustrates the time response of the angular velocity of the pendulum for different pendulum masses

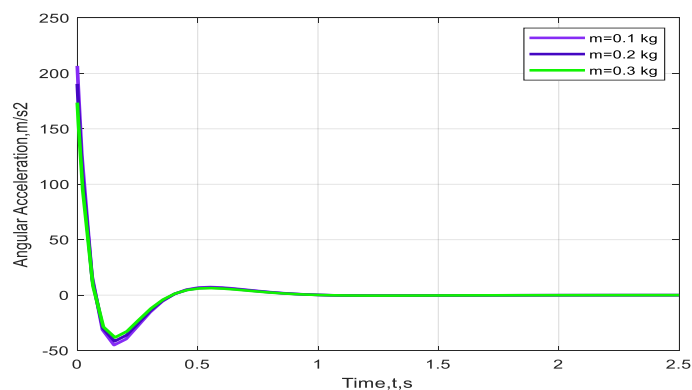


Figure 25. Shows the time response of the angular acceleration of the pendulum for varying pendulum masses

7.3 Effect of the damping coefficient (d)

The time responses of the system at different damping coefficients are presented in this section, as shown in Figures (26-31). The damping coefficients showed nonlinear behavior of the time response of the system. The dynamic responses vary nonlinearly due to the dependency of the damping force on both absolute and relative velocities of the system components. However, the dynamic response show lower sensitivities to the damping

variations of compared with effect of the above parameters (mass of car and pendulum). Small variations in frequency of the dynamic response are noticed in light of the range of damping variations from 0.1-0.3.

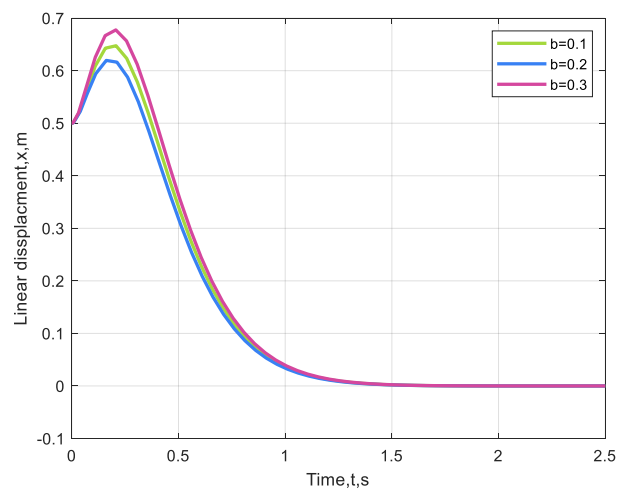


Figure 26. Illustrates the time response of the linear displacement of the cart for varying damping coefficients

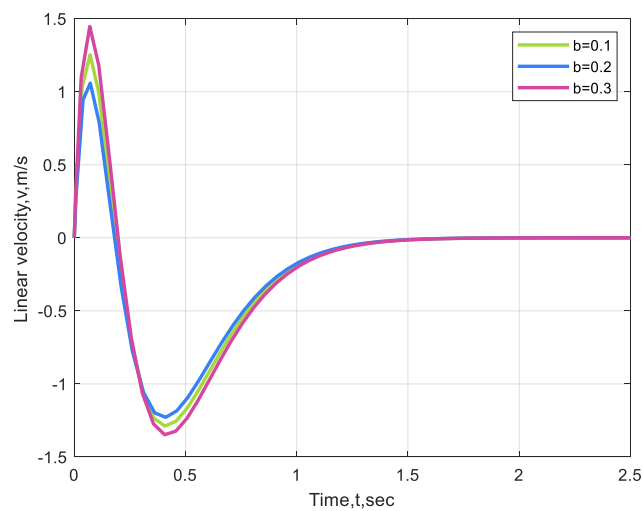


Figure 27. Depicts the time response of the linear velocity of the cart for different damping coefficients

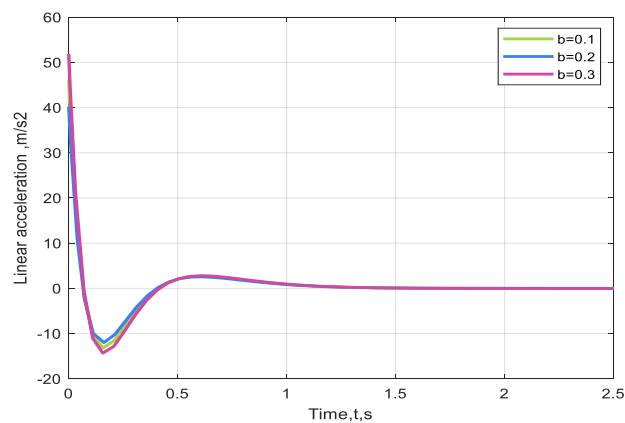


Figure 28. Shows the time response of the linear acceleration of the cart for varying damping coefficients

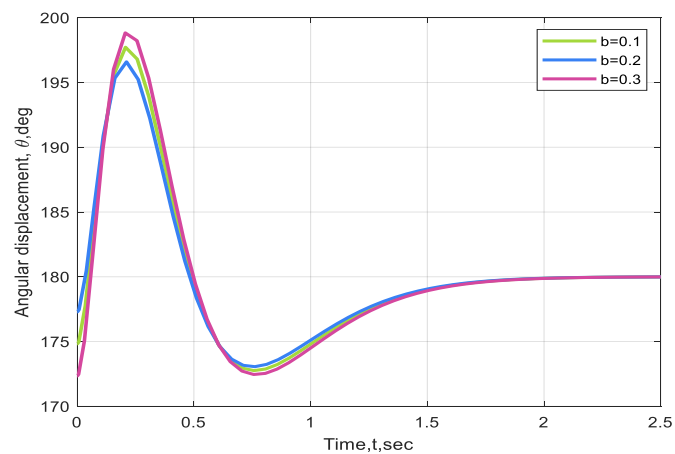


Figure 29. Illustrates the time response of the angular displacement of the pendulum for varying damping coefficients

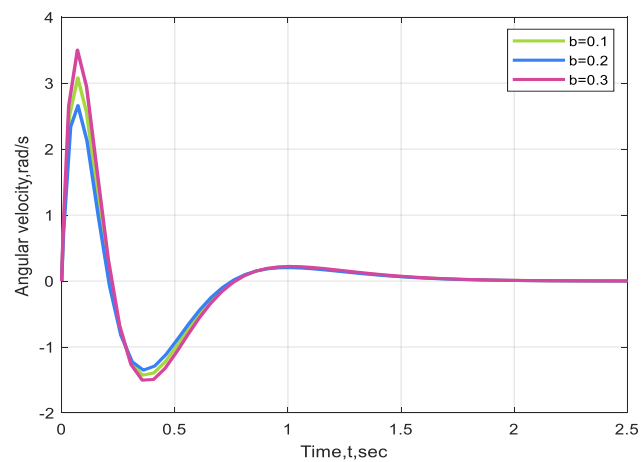


Figure 30. Depicts the time response of the angular velocity of the pendulum for different damping coefficients

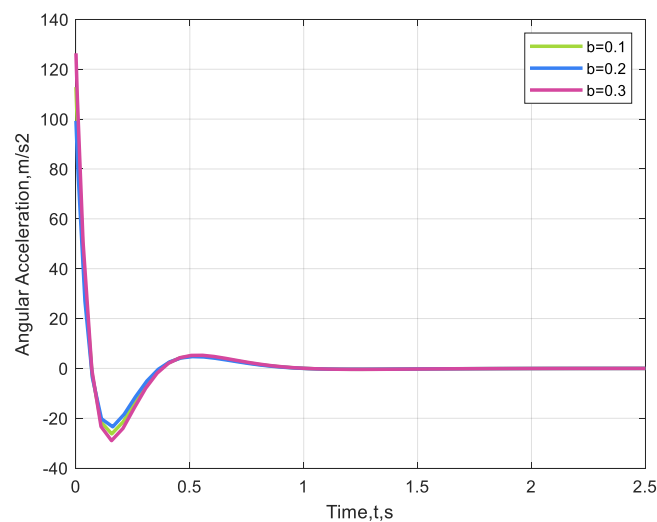


Figure 31. Shows the time response of the angular acceleration of the pendulum for varying damping coefficients

8. Experimental Results

Based on the rig implemented for the experimental test, as explained in the previous chapter, three runs are studied for the cart and pendulum for different initial conditions and constraints. Displacement and velocities of both cart and pendulum are recorded from the accelerometers and processed for good presentations. First of all, the dynamic response of the system is affected by the initial conditions and the tracking point to get the steady state response. Due to experimental limitations, there are only three experimental tests for the system response.

It is not easy to make a direct comparison between the experimental and theoretical results in our test rig because of the difficulties of controlling the nonlinear effect of damping due to its nonlinear nature. However, the results give good explanations about the controllability of the inverted pendulum in terms of system uncertainty. The main objective of these runs is to check if the suggested controller can lead the inverted pendulum system to stability point when the initial conditions vary. Figure 32, shows that the cart started from a position of (-0.1) and ended at the position of 0.2 as steady-state response in duration of 1 sec only. This time is required to lead the inverted pendulum from its unstable angular position (160 deg.) into the steady-state angular position of (180 deg.) in 1 sec as well. It is important to notice that the steady state time of 1 sec is comparable to that corresponding of the almost all theoretical results mentioned above. This agreement can be considered as a good indication about the validity of the results.

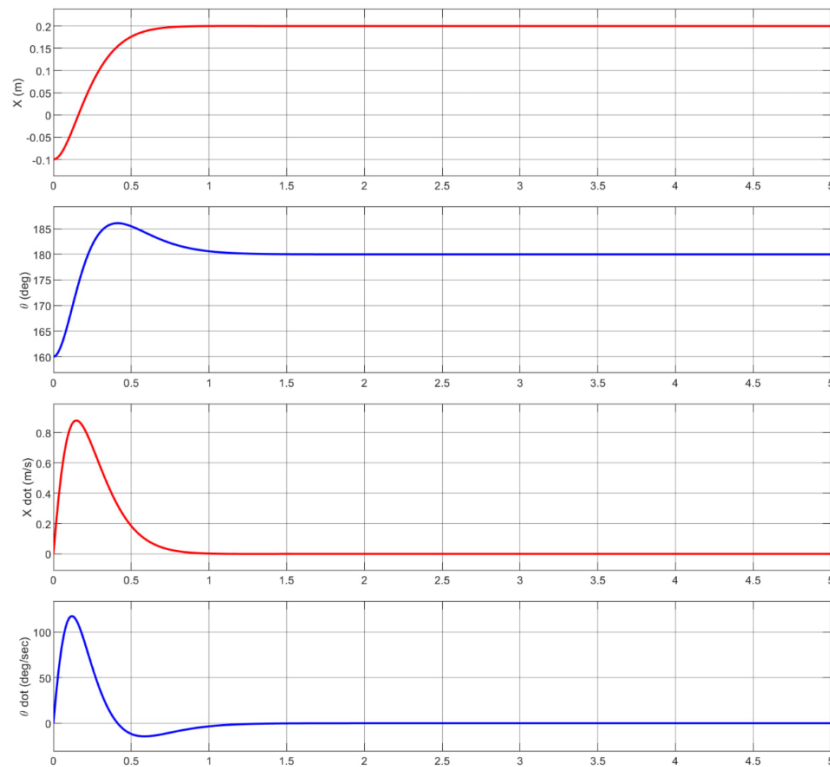


Figure 32. Linear and angular displacement and velocities of the system (experimental work)

However, the situation is different if the stability requirements are different. For example, different behavior is noticed in Fig. 33 where the tracking positions for both cart and pendulum is changed. The cart must be retained to the same position started from (0 m to 0 m position) and (180 deg. to 180 deg. angular position) for the pendulum. Longer time is needed by the cart and the pendulum to return back to the steady state positions. This results is logical since in order to overcome the complex dynamics of the system and interaction in the dynamic response of both cart and pendulum instantaneously, as noticed in the experimental work during running the experiment. The control of the pendulum is seemed to be harder to be controlled because of the centrifugal force

generated that affect the dynamics of cart itself and so on. Eventually, the controller maintained the steady state response after 8 sec for the cart and pendulum.

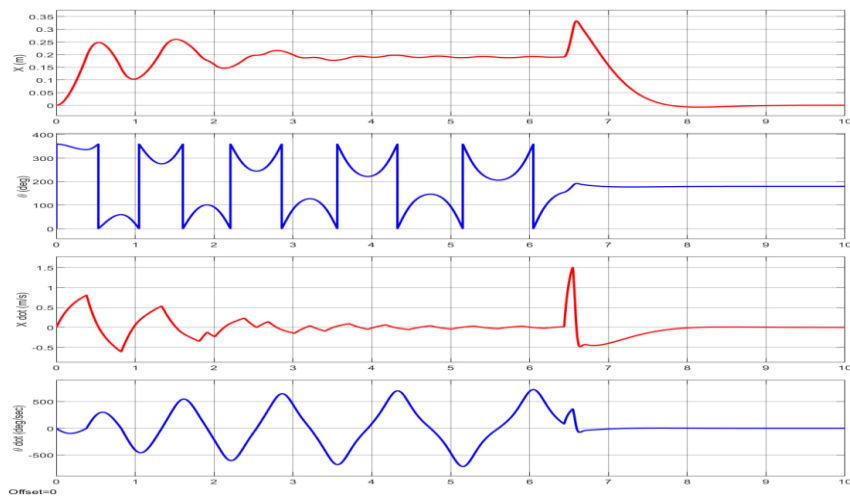


Figure 33. Linear and angular displacement and velocities of the system (experimental work)

Another case of control is studied where the cart requirements are similar to Figure 33, but the pendulum must get the steady state position (180 deg). Smaller time needed to maintain the steady state response where the inverted pendulum started from lower initial angular position. The dynamic response of the linear and angular displacements and velocities of both cart and pendulum are similar in behavior. However, the response of cart directed to the left side of the steady state position to the maximum amplitude value of 0.45 m and retain back to the zero steady state position. Only 7 sec. needed to control the system as shown in Figure 34.

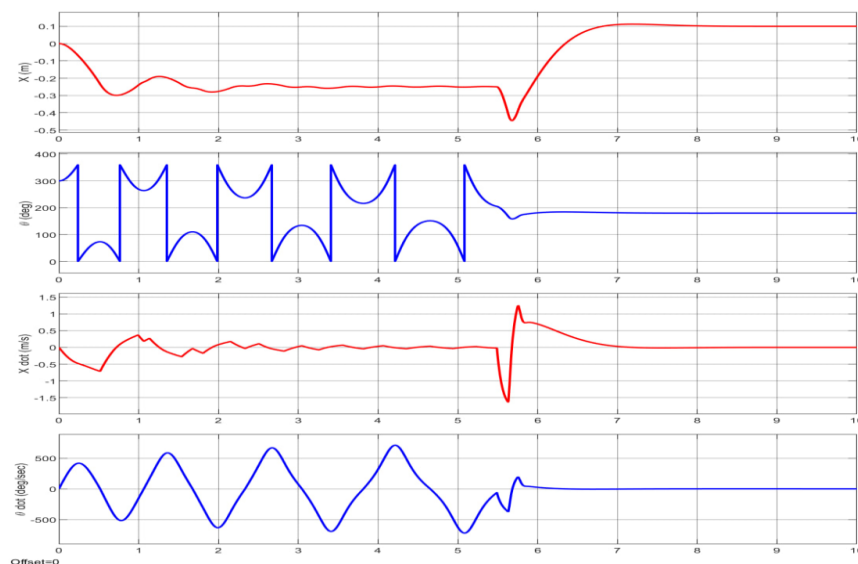


Figure 34. Linear and angular displacement and velocities of the system (experimental work)

9. Conclusion

Based on the results and their discussion, one can conclude that the theoretical work has established the effectiveness of both control methods in supervisory the two masses of the system to the desired values within a short time frame. The LQR method showed a smaller overshoot compared to the Pole Placement Method (PPM) in the linear displacement response, and also attained a quicker steady-state time. The linear velocity responses

also differed between the two approaches. The PPM exhibited a smaller response for the linear velocities compared to the corresponding LQR response. However, the LQR method was intelligent to attain a faster overall response than the PPM. The PPM required less control effort to monitor the angular position of the pendulum to the desired positions in tandem. Monte-Carlo simulations have confirmed the robustness of the controllers, as they successfully drove the system to steady-state conditions across a wide range of initial conditions and system parameter variations, over 50 test runs. Variations in the carts mass prejudiced the overshoot of the time response, but the steady-state time remained mainly unaffected (around 1.67 seconds). The direction of change in the time response was not necessarily proportional to the mass variation, due to the inertial forces acting on the cart. The dynamic response exhibited minor sensitivities to variations in the damping parameters compared to the special effects of the mass parameters.

In the experimental work, the inverted pendulum was positively directed from its unstable angular position of 160 degrees to the steady-state position of 180 degrees in just 1 second. The 1-second steady-state time detected in the experimental work bring into line well with the theoretical results, providing a strong confirmation for the overall findings. Smaller time was essential to retain the steady-state response when the inverted pendulum ongoing from a lower initial angular position.

References

- [1] P. Priyadarshi, "Optimal Controller Design for Inverted Pendulum System : An Experimental Study Department of Electrical Engineering Optimal Controller Design for Inverted Pendulum System : An Experimental Study Master of Technology," 2013.
- [2] J. S. Sham, M. I. Solihin, F. Heltha, and H. Muzaiyanah, "Modelling and simulation of an inverted pendulum system: Comparison between experiment and CAD physical model," *ARPN J. Eng. Appl. Sci.*, vol. 10, no. 20, pp. 9752–9757, 2015.
- [3] S. Jadlovská and J. Sarnovský, "Modelling of classical and rotary inverted pendulum systems - A generalized approach," *J. Electr. Eng.*, vol. 64, no. 1, pp. 12–19, 2013, doi: 10.2478/jee-2013-0002.
- [4] M. Sekiguchi, T. Sugasaka, and S. Nagata, "Control of a multivariable system by a neural network," *Proc. - IEEE Int. Conf. Robot. Autom.*, vol. 3, no. April, pp. 2644–2649, 1991.
- [5] E. M. Ramírez, "Study and design of the control system of an inverted pendulum," no. January, 2018.
- [6] C. Frederickson, R. Sbresny, N. Felker, and A. Getler, "Implementation of an Inverted Pendulum PID Control System Using a Stepper," no. December, 2016, doi: 10.13140/RG.2.2.34564.12164.
- [7] Y. Wang, "Masters Thesis: Optimal Swing-Up Control of an Inverted Pendulum."
- [8] S. Chakraborty, "An Experimental study for Stabilization of Inverted Pendulum," 2014.
- [9] I. Kafetzis and L. Moysis, "Inverted Pendulum: A system with innumerable applications Inverted Pendulum," 9th Int. Week Dedic. to Maths. Thessaloniki, Greece, March 2017., no. February, p. 13, 2017.
- [10] C. Mahapatra and S. Chauhan, "Tracking control of inverted pendulum on a cart with disturbance using pole placement and LQR," 2017 Int. Conf. Emerg. Trends Comput. Commun. Technol. ICETCCT 2017, vol. 2018-Janua, pp. 1–6, 2018, doi: 10.1109/ICETCCT.2017.8280311.
- [11] A. Samuel Ávila Balula, J. Manuel Lage de Miranda Lemos Horácio João Matos Fernandes, L. Filipe Moreira Mendes Supervisor, and J. Manuel Lage de Miranda Lemos, "Nonlinear control of an inverted pendulum Engineering Physics Examination Committee," no. September, 2016.
- [12] Q. Qi, D. Deng, F. Liu, and Y. Tang, "Stabilization of the double inverted pendulum based on discrete-time model predictive control," *IEEE Int. Conf. Autom. Logist. ICAL*, no. August, pp. 243–247, 2011, doi: 10.1109/ICAL.2011.6024721.
- [13] O. Boubaker, "The inverted pendulum: A fundamental benchmark in control theory and robotics," 2012 Int. Conf. Educ. e-Learning Innov. ICEELI 2012, 2012, doi: 10.1109/ICEELI.2012.6360606.

- [14] “The Inverted Pendulum in Control Theory and Robotics: From theory to new innovations,” *Invert. Pendul. Control Theory Robot. From theory to new Innov.*, 2017, doi: 10.1049/pbce111e.
- [15] V. Šetka, R. Čečil, and M. Schlegel, “Triple inverted pendulum system implementation using a new ARM/FPGA control platform,” *2017 18th Int. Carpathian Control Conf. ICCC 2017*, pp. 321–326, 2017, doi: 10.1109/CarpathianCC.2017.7970419.
- [16] I. Hassanzadeh, A. Nejadfard, and M. Zadi, “A multivariable adaptive control approach for stabilization of a cart-type double inverted pendulum,” *Math. Probl. Eng.*, vol. 2011, 2011, doi: 10.1155/2011/970786.
- [17] M. I. Solihin and R. Akmeliawati, “Particle Swarm Optimization for Stabilizing Controller of a Self-erecting Linear Inverted Pendulum,” vol. 3, no. June, pp. 1–9, 2010.
- [18] Wende Li; Hui Ding; Kai Cheng, “An investigation on the design and performance assessment of double-PID and LQR controllers for the inverted pendulum,” 2012.
- [19] J. Kumar, V. E. , Jerome, “An adaptive particle swarm optimization algorithm for robust trajectory tracking of a class of under actuated system,” *Arch. Electr. Eng.*, vol. Vol. 63, pp. 345–365, 2014.
- [20] X. Diao, “Modular control of a rotary inverted pendulum system,” *ASEE Annu. Conf. Expo. Conf. Proc.*, vol. 2016-June, 2016, doi: 10.18260/p.25750.
- [21] J. J. Wang, “Simulation studies of inverted pendulum based on PID controllers,” *Simul. Model. Pract. Theory*, vol. 19, no. 1, pp. 440–449, 2011, doi: 10.1016/j.simpat.2010.08.003.
- [22] E. A. T. 3 Mustefa Jibril 1 Messay Tadesse 2, “Comparison of a Triple Inverted Pendulum Stabilization using Optimal Control Technique,” *Int. J. Electr. Power Eng.*, vol. 14, no. 6, pp. 60–67, 2020, doi: 10.7537/marsroj121020.10.
- [23] R.SOWJANYA AND G. RAMESH, Comparison of a Triple Inverted Pendulum Stabilization using Optimal Control Technique, *Int. J Emerg. Eng. Sci. Technol.*, 1 (2015), pp. 261-265.